

Evangelos Christodoulou · Wojciech R. Rypniewski
Constantinos E. Vorgias

High-resolution X-ray structure of the DNA-binding protein HU from the hyper-thermophilic *Thermotoga maritima* and the determinants of its thermostability

Received: 3 June 2002 / Accepted: 16 October 2002 / Published online: 12 December 2002
© Springer-Verlag 2002

Abstract The histone-like DNA-binding proteins (HU) are a convenient model for studying factors affecting thermostability because of their relatively simple, easily comparable structures, their common function, and their presence in organisms of widely differing thermostability. We report the determination of the high-resolution structure (1.53 Å) at 273 K and 100 K of the HU protein from the hyper-thermophilic eubacterium *Thermotoga maritima* (HUT_{mar}, $T_m = 80.5$ °C). The structural data presented clearly show that the HUT_{mar} has a fold similar to its thermophilic homologue HU from *Bacillus stearothermophilus* (HUB_{st}). Based on primary structure analysis, as well as on the results of mutational analysis of HUB_{st} ($T_m = 61.6$ °C) and *Bacillus subtilis* (HUB_{su}, $T_m = 39.7$ °C), we have designed and produced several single and combined mutations to study their effect on the thermostability of the recombinant HUT_{mar}. Among others, the triplet mutant HUT_{mar}-G15E/E34D/V42I ($T_m = 35.9$ °C) has converted the extreme thermophilic protein HUT_{mar} to mesophilic, like HU B_{su}. In an attempt to analyze the various mutants of HUT_{mar}, we crystallized the point mutation HUT_{mar}-E34D, in which Glu34 was replaced by Asp, similar to the mesophilic HUB_{su}. The mutant has $T_m = 72.9$ °C, as measured by circular dichroism, 7.6 °C lower than the

wild type. The crystal structure of HUT_{mar}-E34D was determined at 100 K and refined at 1.72 Å resolution. A comparison with the wild-type structures clearly shows that two hydrogen bonds have been disrupted between Glu34 from one subunit and Thr13 from the other subunit, and vice versa. Our analysis points to this as the prime cause of the destabilization compared to the wild type. The three new structures were compared, together with the X-ray structure of a similar protein, HUB_{st}, with the aim of relating their structural properties and different thermal stability. The presented results show that the HUT_{mar} protein achieves its stability by employing a dual strategy. On the one hand, we observe local hydrophobic interactions, which stabilize the secondary structure elements, and on the other hand, electrostatic interactions between side chains.

Keywords *Thermotoga maritima* · Hyper-thermostable histone-like protein HU · X-ray structure · Mutants

Communicated by G. Antranikian

PDB references: HUT_{mar}-wt (277 K) 1b8z; HUT_{mar}-wt (100 K) 2b8z; HUT_{mar}-E34D (100 K) 3b8z.

E. Christodoulou · C.E. Vorgias (✉)
National and Kapodistrian University of Athens,
Faculty of Biology, Department of Biochemistry
and Molecular Biology, Panepistimiopolis-Zographou,
157 84 Athens, Greece
E-mail: cvorgias@biol.uoa.gr
Tel.: +30-210-7274514
Fax: +30-210-7274158

W.R. Rypniewski
Institute of Biochemistry and Molecular Biology,
UKE, c/o DESY, Build.22a, Notkestrasse 85,
22603 Hamburg, Germany

Introduction

The eubacterial cell nucleoid contains a number of abundant, small, basic proteins classified as histone-like DNA-binding proteins. Among these proteins, HU has been identified as the major and ubiquitous protein component of the bacterial nucleoid. In *E. coli*, HU (HU $\alpha\beta$) is the most abundant DNA-binding protein, with ~30,000 dimers per cell. It is a heterodimer consisting of two (70% identity) subunits, α and β , each 90 amino acids long, encoded by the genes *hupA* and *hupB*, respectively. HU appears to be a homodimer in nearly all bacterial species where it has been studied, except in *E. coli*, *Serratia marcescens*, and *Salmonella typhimurium*. A comprehensive review on HU has been published (Drlica and Rouvière-Yaniv 1987; Pettijohn 1988). Nearly 100 HU genes have been identified and deposited in the databanks.

HU binds with low sequence specificity to both single-stranded and double-stranded DNA as well as RNA (Rouvière-Yaniv and Gros 1975). HU binds preferentially

to cruciform DNA and DNA-specific structures induced by supercoiling, nicks, and gaps and causes DNA bending and negative supercoiling. Furthermore, HU interacts with DNA, forming condensed nucleosome-like particles, and can introduce negative supercoiling into a relaxed circular plasmid DNA in the presence of topoisomerase I (Rouvière-Yaniv et al. 1979; Broyles and Pettijohn 1986).

In its accessory function, HU is involved in a number of other protein-DNA interactions such as binding of the *lac* repressor and facilitating the binding of the cAMP receptor protein to the *lac* promoter (Flashner and Gralla 1988). HU is a required factor in the transposition by bacteriophage Mu (Craigie et al. 1985) and plays, in vitro, a regulatory role in λ DNA replication (Mensa-Wilmot et al. 1989). HU is an important component of transposons and forms tight complexes in four-way junction DNA. *E. coli* HU α , and HU β are regulated by CRP and FIS proteins (Claret and Rouvière-Yaniv 1996). It has also been reported that HU binds specifically to DNA that contains single-strand breaks or gaps (Castaing et al. 1995) and, recently, that HU binds to DNA, forming multiple complexes, and bends DNA (Wojtuszewski et al. 2001; Grove and Lynette 2001).

The crystal structure of HU from *B. stearothermophilus* (HUBst) has been solved (Tanaka et al. 1984) and recently refined at 2 Å (White et al. 1999). The solution structure of the recombinant HU from *B. stearothermophilus* expressed in *E. coli* (Padas et al. 1992) has also been determined by NMR (Vis et al. 1995; Boelens et al. 1996). HUBst protein has been used as a model system to study protein-DNA interaction(s) of the histone-like protein family that includes the integration host factor (IHF) protein (Rice et al. 1996; White et al. 1989).

The structural properties responsible for the thermostability of HU proteins from mesophilic and thermophilic microorganisms attracted attention in the past (Wilson et al. 1990). Meanwhile, the HU proteins from *B. stearothermophilus* and *B. subtilis* have been analyzed with respect to their sequence characteristics in correlation with their thermostability (Christodoulou and Vorgias 2002; Kawamura et al. 1996, 1998). We want to expand our studies on the HU protein to extreme thermophilic organisms, such as the eubacterium *T. maritima* (growth temperature 80–85 °C), which shows 61% and 51% identity to HU from the thermophilic *B. stearothermophilus* and the mesophilic *B. subtilis*, respectively. The small size of the HU molecule and the existence of homologous proteins in various bacteria, from mesophilic to extreme thermophilic, make it an attractive model to address questions of thermostability using the structure-mutation approach.

Engineering proteins for thermostability is a particularly exciting and challenging field, as it is crucial for broadening the industrial use of recombinant proteins. Many experimental approaches have been applied to identify determinants of thermostability (Zuber 1988; Serrano et al. 1993; Shih and Kirsch 1995; Spector et al.

2000; Sriprapundh et al. 2000). The structure-mutation approach was applied predominantly, but it is time-consuming and expensive and requires proteins that are highly conserved in their primary structure and are present in organisms that grow at low and high temperatures (Steen et al. 2001). Therefore, only a limited number of proteins have been studied based on this approach (Salminen et al. 1996; Lehmann and Wyss 2001).

The comparison of homologous proteins with different thermostabilities offers a unique opportunity to elucidate strategies for thermal adaptation. Despite their widely different thermostabilities, thermophilic proteins and their mesophilic counterparts often share the same function, high-sequence homology, and similar three-dimensional structure (Kumar et al. 2000). Thermostability in various thermostable proteins seems not to be achieved by a single universal mechanism but by a combination of individual strategies, such as an increased number of hydrogen bonds and salt bridges, an optimized packing of the hydrophobic core, shortened surface loops, increased number of proline residues, and an increase in buried hydrophobic residues (Querol et al. 1996; Jaenicke and Böhm 1998; Ladenstein and Antranikian 1998; Sterner and Leibl 2001).

The present work is based on the principle of rational design and focuses on studies of structure-thermostability using X-ray structural analysis in combination with primary structure analysis and targeted site-directed mutagenesis using as a model system the DNA-binding protein HU from microorganisms living in a wide range of temperatures. The purpose of our study is to identify the molecular determinants responsible for the hyperthermostability of the HUTmar protein.

Materials and methods

Cloning, expression, and purification

The cloning, expression, and purification of the HUTmar has been described previously (Christodoulou and Vorgias 1998). Site-specific mutagenesis, using asymmetric PCR with a single mutagenic primer and two flanking primers, was performed to produce the HUTmar-E34D mutation as described by Perrin and Gilliland (1990). The synthetic oligonucleotides used were a 28-mer 5' ACATATGAACAAGAAGGAAGCACTCATCGAC 3' HUTmar(C), a 29-mer 5' AGGGATCCTCACTTGACCTTCTCTTTGAG 3' HUTmar(N), and a 44-mer 5' AATCCAACGATCTGAACCTTTCACCCTTTGCGAGAGCGTCTGT 3' HUTmar(C)E/D. All procedures used for cloning, expression, and purification of the HUTmar-E34D mutant protein were the same as for the wild type.

Protein sequence alignment

The sequences of several HUs, selected according to growth temperature of the parent organisms, were aligned using Clustal X (Thompson et al. 1997).

Amino acid analysis

For ease of presentation, each amino acid was assigned to one of three categories: charged (Asp, Glu, Arg, and Lys), uncharged

polar (Ser, Thr, Asn, and Gln), and non-polar (Gly, Ala, Val, Leu, Ile, Phe, Trp, Tyr, Pro, Met, Cys, and His) (Haney et al. 1999).

Crystallization of *HUTmar* wild type and mutant

The crystallization and production of high-quality crystals of *HUTmar* wild-type (wt) and mutant E34D were carried out under identical conditions using the vapor diffusion method as described previously (Christodoulou and Vorgias 1998). *HUTmar*-wt and *HUTmar*-E34D formed crystals in 80% saturated ammonium sulfate, at room temperature, after 3–5 months, and the obtained crystals have tetragonal symmetry.

Circular dichroism spectroscopy

Circular dichroism (CD) spectroscopy experiments were conducted using a JASCO 715 spectropolarimeter with a Peltier-type cell holder (model PTC-348 from Jasco Corporation), which permits accurate temperature control. Wavelength scans were performed using 0.2 mg/ml protein concentration in a 2-mm rectangular cell at a number of discrete temperatures. The proteins were dissolved in 10 mM MOPS pH 7.0. Each spectrum was obtained by averaging four spectra recorded from 250 to 190 nm with 2-nm intervals at the rate of 50 nm min⁻¹. A response time for each point was 5 s and the bandwidth was 2 nm. Buffer scans were accumulated and subtracted from the sample scans, and the mean residue ellipticity was calculated. CD temperature scans were performed by varying the temperature from 20 to 95 °C at a rate of 50 °C h⁻¹, and the mean ellipticity was measured at 222 nm with 0.5 °C intervals, 5 s response time, and 2 nm bandwidth. The protein concentration was 0.2 mg/ml. Both wild type and mutants were examined reversibly under these experimental conditions. The fraction of native protein was calculated from the CD values by linearly extrapolating the pre- and post-transition baselines, respectively, based on the assumption that the unfolding equilibrium of these proteins follows a two-state mechanism. The temperature of the midpoint of the transition, T_m , at which half of the protein is unfolded, was determined using the sigmoidal fitting of Boltzmann's equation.

X-ray data collection and processing

X-ray diffraction data were collected using synchrotron radiation on the EMBL beam lines X11 and BW7B (van Silfhout and Hermes 1995) at the DORIS storage ring, DESY, Hamburg, on a MAR Research imaging plate scanner. Datasets were collected from single crystals at 277 K and at 100 K for *HUTmar*-wt and at 100 K for the mutant *HUTmar*-E34D. The oscillation angle was varied to minimize the overlapping of reflections. A range of reciprocal space of 100° was covered in two separate sweeps, at different exposure times, for both *HUTmar*-wt and *HUTmar*-E34D, to record the full range of intensities. The programs DENZO and SCALEPACK (Otwinowski and Minor 1997) were used for data reduction and scaling. Initial scaling showed that no significant radiation damage had taken place during data collection and that the images were scaled without a relative temperature factor. Outliers were rejected based on the χ^2 test implemented in SCALEPACK. The post-refinement option was used to refine the cell parameters. The intensities were converted to structure factor amplitudes, and a correction was applied to weak or negative measurements (French and Wilson 1978). Data collection and the final statistics are summarized in Table 4.

Structure determination and refinement

The structure of *HUTmar*-wt at 277 K was determined by molecular replacement using the program AMORE (Navaza 1994) from the CCP4 program suite (Collaborative Computational Project Number 4 1994). The rotation function was calculated using terms

between 8 and 3 Å with a Patterson search radius of 20 Å. Using the structure of HU from *B. stearothermophilus* refined at 1.9 Å as the starting model, a solution was obtained (Dauter Z., personal communication) and placed in a P1 cell of dimensions 80×80×80 Å. A peak in the rotation function was obtained, giving a correlation coefficient of 0.199, while the other peaks had height less than 55% of this peak. It was not clear at that stage whether the space group was P4₁ or P4₃, and the translation function was calculated for both space groups using the orientation corresponding to the highest peak found in the rotation function. The translation function gave a peak with a correlation coefficient of 0.208 and an R factor ($= \sum |F_o|/F_c|/\sum F_o$) of 0.566 for space group P4₁, while P4₃ gave a correlation coefficient of 0.382 and an R factor of 0.49. This was further improved by rigid body refinement, as implemented in AMORE, to give a correlation coefficient of 0.425, with an R factor 0.476. The model was refined by the conventional stereochemically restrained maximum-likelihood method (Murshudov et al. 1999) as implemented in the program REFMAC from the CCP4 program suite. Data were used between 20 and 1.6 Å, without a σ cutoff, with 5% of the dataset aside for R_{free} (Brünger 1992). Solvent molecules were inserted and refined using the program ARP (Lamzin and Wilson 1993) with real space positional refinement and automatic determination of statistically significant electron density level. Manual rebuilding of the model was based on the ($2F_o - F_c$) and ($F_o - F_c$) electron density maps, using an SGI graphics station and O (Jones et al. 1991).

The model of *HUTmar*-wt at 100 K also was refined by using the refined coordinates of *HUTmar*-wt at 277 K as a starting model, and the refinement was performed as described above. Diffraction data used were between 20 and 1.53 Å.

The model of *HUTmar*-E34D at 100 K was also refined by using the structure of *HUTmar*-wt at 277 K as the starting model. Data used were between 20 and 1.72 Å.

Results

Comparison of HU proteins from microorganisms living at various temperatures

HU proteins from four bacteria and the first archaeon that contains HU protein have been selected for comparison studies based on their growth temperature. The characteristics of the microorganisms and some available biochemical data concerning the HU proteins are summarized in Table 1.

Primary and secondary structure comparison of the HU proteins

As a first step to understanding and explaining the molecular basis of the thermostability of the selected HU proteins, primary and secondary structure comparisons were performed among the mesophilic *HUBsu*, thermophilic *HUBst* and *HUTvo* (Kawashima et al. 2000), and extreme thermophilic *HUTth* and *HUTmar*. The topology of the *HUBst* protein is described in White et al. (1999). The topology of *HUTmar* is described later in this report in the section on X-ray structure determination.

In a previous publication (Christodoulou and Vorgias 2002), we proposed to divide the topology of the HU molecule into three “domains” based on functional considerations rather than structural. For each monomer

Table 1 Comparison of the five HU proteins selected according to their growth temperatures (several other statistical data are also presented)

| Parameter Organism | HUBsu <i>Bacillus subtilis</i> | HUBst <i>Bacillus stearothermophilus</i> | HUTvo <i>Thermoplasma volcanium</i> | HUTth <i>Thermus thermophilus</i> | HUTmar <i>Thermotoga maritima</i> |
|--------------------------------------|-----------------------------------|---|--|--|--|
| Growth temperature (°C) | 30 | 55 | 60 | 70 | 80 |
| Databank entry | O31946 | P02346 | BAB59303 | P19436 | P36206 |
| Number of amino acids in the monomer | 92 | 90 | 90 | 95 | 90 |
| T_m of the protein (°C) | 39.7 | 61.6 | 60.0 | n.d. | 80.5 |
| Charged residues (%) | 32.5 | 33.4 | 28.9 | 31.6 | 38.9 |
| Uncharged residues (%) | 17.3 | 16.7 | 24.5 | 14.8 | 11.1 |
| Nonpolar residues (%) | 50.2 | 49.9 | 46.6 | 53.6 | 50.0 |
| Homodimer (Da) | 19.782 | 19.420 | 20.056 | 20.312 | 19.972 |
| X-ray structure available | - | 1HUUA, 1HUUB, 1HUUC | - | - | 1B8ZA, 1B8ZB |

Table 2 Identity scores among the HUBsu, HUBst, HUTth, and HUTmar proteins and their domains^a

| | HUBsu | HUBst | HUTvo | HUTth | HUTmar |
|--------|------------|------------|------------|------------|--------|
| HUBsu | 100.0% | | | | |
| HUBst | 87.7% | 100.0% | | | |
| | HTH: 77.8% | | | | |
| | DBD: 100% | | | | |
| HUTvo | 35.9% | 32.6% | 100.0% | | |
| | HTH: 28.9% | HTH: 24.4% | | | |
| | DBD: 37.5% | DBD: 35.0% | | | |
| HUTth | 51.1% | 55.5% | 24.4% | 100.0% | |
| | HTH: 35.5% | HTH: 44.4% | HTH: 17.8% | | |
| | DBD: 65.0% | DBD: 90.6% | DBD: 25.0% | | |
| HUTmar | 51.1% | 61.1% | 33.3% | 55.5% | 100.0% |
| | HTH: 33.0% | HTH: 53.3% | HTH: 26.7% | HTH: 44.4% | |
| | DBD: 67.5% | DBD: 67.5% | DBD: 35.0% | DBD: 65.0% | |

^a Helix-turn-helix body (HTH): (residues: 1–45) and DNA binding domain (DBD): (residues: 51–90). The DS peptide is not included since it is identical among all known HUs

of the HU molecule, we can distinguish the helix-turn-helix (HTH) domain, the dimerization signal (DS), and the DNA-binding domain (DBD), which is comprised of the flexible arm and a small α -helix. Figure 1 presents the primary structure alignment of the HUs described in Table 1. The secondary structure elements described in Fig. 1 are derived from the X-ray structure of HUBsu, HUBst, and HUTmar but cannot be assigned accurately for HUTvo and HUTth.

The HU proteins of the five organisms used in this study (Table 1) and their HTH and DBD parts were compared and expressed as percent of identity. The resulting calculations are presented in Table 2. The DS signal was not included in Table 2, since it is practically identical in all HU proteins.

Mutational analysis

An extensive mutational analysis has been carried in the HUBsu, HUBst, and HUTmar proteins in order to assess the contribution of certain highly conserved amino acids and shed light on the mechanism of thermostabilization of these proteins (Christodoulou and Vorgias 2002).

The study points to three amino acids being primarily responsible for the thermal stability of these HU proteins. They are Gly15, Glu34, and Val42 in HUBsu, HUBst, and HUTmar. However, these results cannot be

extrapolated for HUTth and HUTvo, as there are no available data for their structures. Gly15, Glu34, and Val42 in HUTmar were mutated to their mesophilic counterparts, individually and in combination. The mutated HUTmar proteins were overexpressed in *E. coli* and purified to homogeneity (Christodoulou and Vorgias 1998), and their melting temperature was determined by CD spectroscopy. Fig. 2a presents the full CD-spectrum of HUTmar-wt at various temperatures, and Fig. 2b shows the melting curves of the HUTmar-wt and the mutants described in Table 3. The experimentally determined T_m of the HUTmar-wt and various mutants and the localization of the mutated amino acids onto the three-dimensional structure of HUTmar are summarized in Table 3.

Crystallization experiments

As the next step, we decided to determine the X-ray structure of the HUTmar-wt and the available mutants in order to understand the mechanism of HUTmar stabilization at the molecular level.

HUTmar-wt was crystallized and the crystals were diffracted to high resolution. The mutant HUTmar-E34D was also crystallized under the same conditions. Crystallization trials are underway to obtain high-quality crystals of HUTmar-G15E, HUTmar-V42I, and the triplet mutant HUTmar-G15E/E34D/V42I to gain

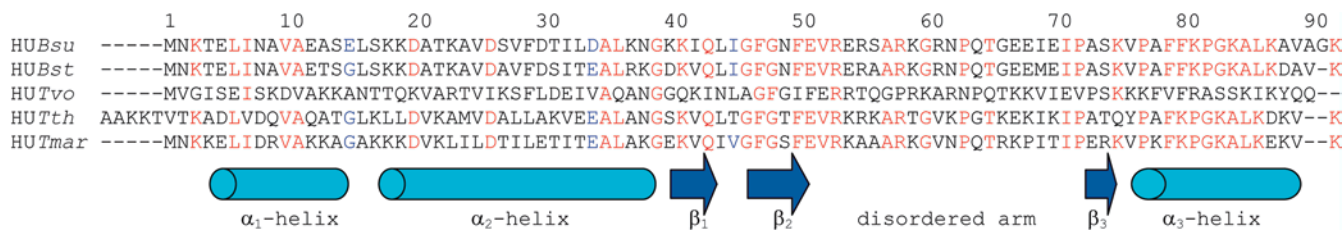


Fig. 1 Alignment of the amino acid sequences of HUBst, HUBgl, HUTvo, HUTth, and HUTmar. The positions of the secondary structure elements derived from the three-dimensional structure of HUBst are shown. α_1 , α_2 , and α_3 are α -helices; β_1 , β_2 , and β_3 are β -sheets; and DS is dimerization signal

additional insight into the structural rearrangements responsible for their reduced thermostability.

Both HUTmar-wt and HUTmar-E34D proteins formed bi-pyramidal crystals in the space group $P4_3$ with a unit cell containing eight HU polypeptide chains arranged as four dimers around the 4_3 axis. Table 4 summarizes the unit cell parameter of the measured crystals of HUTmar-wt and E34D mutant.

The model of HUTmar-wt at 277 K and 100 K and HUTmar-E34D at 100 K

The statistics of data collection for HUTmar-wt at 277 K and 100 K, as well as for HUTmar-E34D at 100 K, are summarized in Table 4. The models of HUTmar-wt based on data collected at 277 K and 100 K consist of 1028 and 978 protein atoms and 67 and 148 solvent molecules, respectively. In the case of HUTmar-E34D mutant, the data were collected at 100 K and the model was built using 975 protein atoms and 89 solvent molecules. Table 5 summarizes the statistics of the three models. The quality and geometry of all three final models, HUTmar-wt at 277 K and 100 K and E34D mutant at 100 K, were analyzed using PROCHECK (Laskowski et al. 1993). The three models do not deviate significantly and are within the accepted limits of various geometrical criteria as summarized in Table 6.

The Ramachandran plot for the HUTmar-wt (Ramachandran and Sasisekharan 1968) is well clustered within the accepted regions and has 98.5% of residues in the most favored region and 0.5% in the additional allowed region, as defined in the program PROCHECK. The only outlying residue is the conserved Phe47, which is involved in aromatic inter-subunit stacking interactions (White et al. 1999). The stereochemical restraints for the three models and the final standard deviations are listed in Table 6.

The structure of HUTmar and the molecular contacts in the homodimer

As mentioned above, the monomer of the HU molecule consists of three parts, the HTH domain, the DS, and

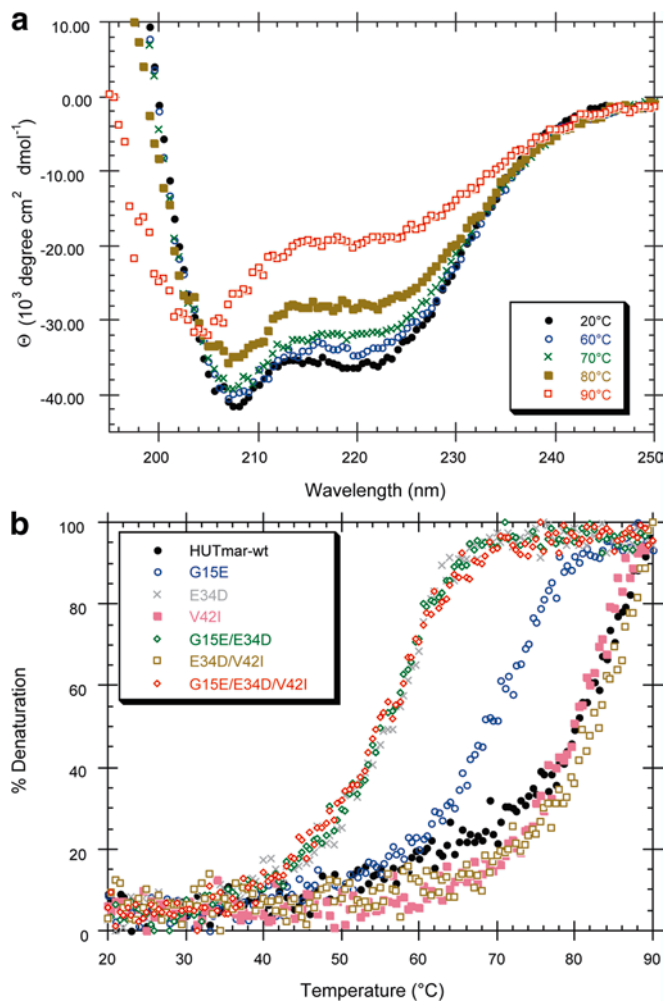


Fig. 2 a UV-CD spectra of HUTmar at various temperatures as indicated on the figure. b Melting curves of HUTmar-wt and mutants indicated on the figure. The experimental conditions are described in Materials and methods

the flexible arm (DBD). In the homodimer, the two HTH domains, the two dimerization signals, and a small three-stranded β -sheet comprise the main body of the molecule. Two short α_3 -helices at the C-end of the molecule are also associated with the main body (Fig. 3). The two flexible arms of the molecule are extended, forming a U-shaped path that is responsible for the binding of the protein to DNA.

The HTH domain is comprised of two helices: α_1 (residues 3–14) and α_2 (residues 18–38) connected via a three-residue short loop (residues 16–17). The primary structure of the HTH domain is not as highly conserved as the DNA-binding domain of the molecule, among all

Table 3 Summary of the wt and mutated HUTmar proteins and their effects on the T_m as determined by CD and their localization on the structure

| From HUTmar to HUBsu | T_m (°C) | ΔT_m (°C) | Secondary structure occurrence of the mutant(s) |
|-------------------------|------------|-------------------|--|
| HUTmar -wt | 80.5 | | |
| G 15 E | 55.8 | -24.7 | Turn between α_1 -helix and α_1 -helix |
| E 34 D | 72.7 | -7.8 | α_2 -helix |
| V 42 I | 70.9 | -9.6 | β_1 -strand |
| G 15 E / E 34 D | 52.1 | -28.4 | Turn between α_1 -helix and α_1 -helix, β_2 -strand |
| E 34 D / V 42 I | 63.4 | -17.1 | Turn between α_1 -helix and α_1 -helix, α_2 -helix |
| G 15 E / E 34 D / V42 I | 35.9 | -44.6 | Turn between α_1 -helix and α_1 -helix, α_2 -helix, β_2 -strand |

Table 4 Statistics of data collection of HUTmar-wt at 277 K and 100 K and HUTmar-E34D at 100 K

| | HUTmar -wt (277 K) | HUTmar-wt (100 K) | HUTmar-E34D (100 K) |
|---|--------------------|-------------------|---------------------|
| Beam line at DORIS | BW7B | X11 | X11 |
| Maximum resolution (Å) | 1.6 | 1.53 | 1.72 |
| Data collection temperature (K) | 277 | 100 | 100 |
| Number of images | 175 | 242 | 258 |
| Oscillation range | 0.8–1.6 | 0.7–1.0 | 1.0 |
| Wavelength (Å) | 0.8833 | 0.905 | 0.9096 |
| R_{merge}^a | 0.056 | 0.044 | 0.050 |
| Raw measurements used | 127,048 | 220,803 | 239,228 |
| Unique reflections | 21,639 | 23,127 | 16,554 |
| Percent completeness | 99.9 | 99.9 | 99.9 |
| Percent completeness in high-resolution bin | 100 | 99.9 | 100 |
| Percent reflections greater than 2σ | 84 | 90.7 | 88.5 |
| Percent reflections greater than 2σ in high-resolution bin | 55 | 73.3 | 65 |
| I/σ in highest resolution bin | 2.7 | 3.4 | 3 |
| Unit cell parameters | | | |
| Space group | P4 ₃ | P4 ₃ | P4 ₃ |
| a = b (Å) | 46.12 | 45.28 | 45.43 |
| c (Å) | 77.56 | 76.17 | 76.45 |

^a $R_{merge} = \sum |I_i| \langle I \rangle / \sum \langle I \rangle$, where I_i is an individual intensity measurement and $\langle I \rangle$ is the average intensity for this reflection with summation of all data

Table 5 Summary of the statistics of the final models of HUTmar-wt at 277 K and 100 K and HUTmar-E34D at 100 K

| | HUTmar-wt (277 K) | HUTmar-wt (100 K) | HUTmar-E34D (100 K) |
|---|-------------------|-------------------|---------------------|
| Protein atoms | 1028 | 978 | 975 |
| Solvent atoms | 67 | 148 | 89 |
| Mean temperature factors main-chain atoms (Å ²) | 23.0 | 25.3 | 29.9 |
| B factor side-chain atoms | 31 | 29 | 34 |
| Co-ordinate error estimate Based on maximum likelihood | 0.06 | 0.06 | 0.08 |
| Final R factor ($= \sum F_o F_c / \sum F_o$) (%) | 22 | 23 | 23 |
| Final R_{free} (%) | 25 | 26 | 26 |

Table 6 Model geometry comparison of the three final HUTmar models

| Distances (Å) | σ^a | HUTmar (277 K) | HUTmar (100 K) | HUTmar -E34D (100 K) |
|------------------------------|------------|----------------|----------------|----------------------|
| rms for bonds ^b | 0.020 | 0.008 | 0.006 | 0.008 |
| rms for bond angle distances | 0.040 | 0.025 | 0.019 | 0.021 |

^a The weights correspond to $1/\sigma^2$

^b rms = root mean square

known HUs, as shown in Table 2. In the dimer of HUTmar, the secondary structure elements are highly intertwined between the subunits. The intersubunit interactions are summarized in Table 7. The intersubunit interactions in HUTmar-E34D and HUBst are also described for comparison.

The dimerization signal is a small part of the molecule (residues 46–50), located partly in the loop between strands β_1 and β_2 and partly on the β_2 -strand, and is highly conserved among the known HU proteins. Phe 29, 47, 50, and 79 from each monomer are involved in the formation of an aromatic hydrophobic core involving

inter-subunit stacking, which fills the space under the saddle like β -sheet region, not only stabilizing the entire homodimer but also triggering the homodimerization of the molecule upon folding (Burley and Petsko 1985). The conformation of all the Phe residues is regular, except for Phe47, which is an outlier on the Ramachandran plot (data not shown).

The β -sheet is formed by the β -strands, β_1 (residues 41–43), β_2 (residues 48–52), and β_3 (residues 76–80), which are well ordered, forming a saddle-like structure. A cartoon of the HUTmar model is shown in Fig. 3.

The flexible arms (residues 53–75) are highly conserved among known HUs and have 22 charged residues in the dimer. The arms are formed at the C-terminal part of the molecule, which is located between the strands β_2 and β_3 . They are very flexible and are mainly responsible

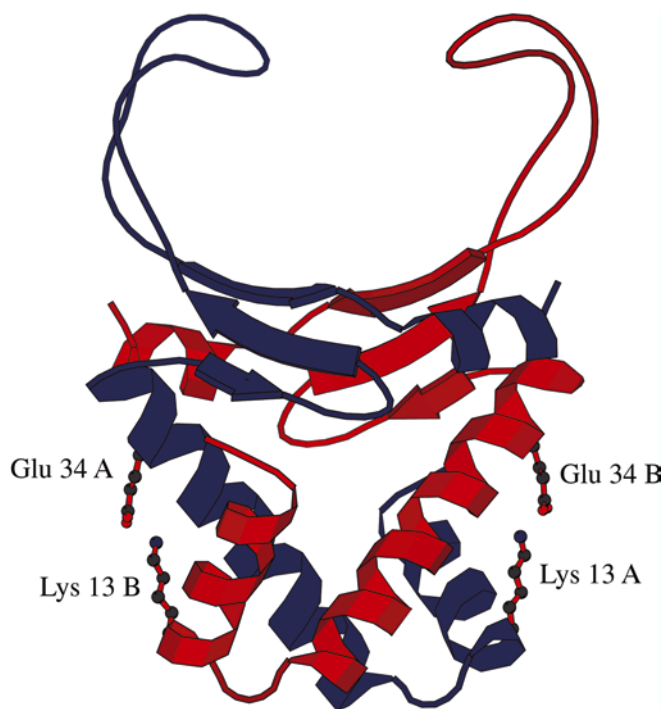


Fig. 3 Ribbon drawing model of the X-ray structure of HUTmar and the location of the Glu34 and Lys13 amino acid residues on the structure. *A* and *B* indicate the corresponding subunits in the homodimer. The cartoon of the structure was made using the program MOLSCRIPT (Kraulis 1991)

Table 7 Overall structural comparison among HUTmar-wt at 277 K and 100 K, HUTmar-E34D at 100 K, HUBst, and IHF

| | rms on C_{α} atoms (Å) | |
|--------------|-------------------------------|---|
| Molecule A/B | 0.04 | For 62 C_{α} atoms |
| HUTmar/cryo | 0.18 | For 126 C_{α} atoms |
| HUTmar/E34D | 0.17 | For 126 C_{α} atoms |
| HUTmar/IHF | 1.2 | For 125 C_{α} atoms |
| HUTmar/HUBst | 0.7 | For chain A 125 C_{α} atoms ^a |
| | 0.7 | For chain B 125 C_{α} atoms |
| | 0.62 | For chain C 125 C_{α} atoms |

^a Chains A, B, and C are the monomer chain in the asymmetric unit

for the binding of the protein to DNA (White et al. 1989, 1999). The flexible arms could not be resolved in either of the three crystal structures being disordered, even at 100 K, although there was good electron density of the rest of the HUTmar molecule.

Finally, the small α_3 -helix (residues 82–89) at the C-terminus of the molecule is associated with the main body of the dimer via interactions with the α_2 -helix of the other subunit.

Comparison of the structures of HUTmar-wt at 277 K and 100 K and HUTmar-E34D at 100 K

The refined atomic models of HUTmar-wt at 277 K and 100 K and the E34D mutant at 100 K were compared to assess the effects of model quality, crystal packing, or cryogenic treatment. Table 7 presents the root mean square (rms) differences in coordinates between least-squares-fitted ordered C_{α} atoms, between subunits, and between different molecules. The structures of the individual HU monomers are very similar, and the differences are within the estimated coordinate error. The three models are also very similar, with differences in the C_{α} s of the same order between the wt at 277 K and 100 K structures and the E34D mutant structure at 100 K. The calculated C_{α} s show no differences greater than three rms. A comparison of dihedral angles formed by four successive C_{α} s did not reveal any major differences in the main chain conformation. The surface area excluded from the solvent upon dimerization was calculated for the HUTmar-wt and the mutant structures and was found to be very similar for all the structures (Table 8).

In the HUTmar-wt structure, Glu34 of chain B makes a salt bridge with Lys13 of chain A. Lys13 also makes an H-bond with Thr31 of chain B. Thr31 is also involved in an intra-subunit H-bond with Thr28. Lys13 of chain B, Glu34, Thr31, and Thr27 of chain A interact with the same H-bond network (Fig. 4a). This H-bond network is clearly shown in Fig. 4b. The effect of the E34D mutation on the structure of the HUTmar-E34D molecule is clearly visible on the least-square-fitted models of wt (in yellow) and E34D mutant (in green) (Fig. 4b). The Asp introduced at position 34 with a shorter side chain no longer makes a salt bridge with Lys13. These two side chains are shifted towards the bulk solvent compared to the wild-type structure. The changes are localized with remarkably little difference in the neighboring residues, as revealed by superimposing the two structures (Fig. 4b) and by comparing the B-factors for these residues.

Table 8 Surface area excluded upon homodimerization of the three final HUTmar models in Å³

| | Chain A (Å ³) | Chain B (Å ³) | Average (Å ³) |
|---------------------|---------------------------|---------------------------|---------------------------|
| HUTmar-wt (277 K) | 584.0 | 572.0 | 578.0 |
| HUTmar-wt (100 K) | 588.0 | 581.0 | 584.5 |
| HUTmar-E34D (100 K) | 576.0 | 586.0 | 581.0 |

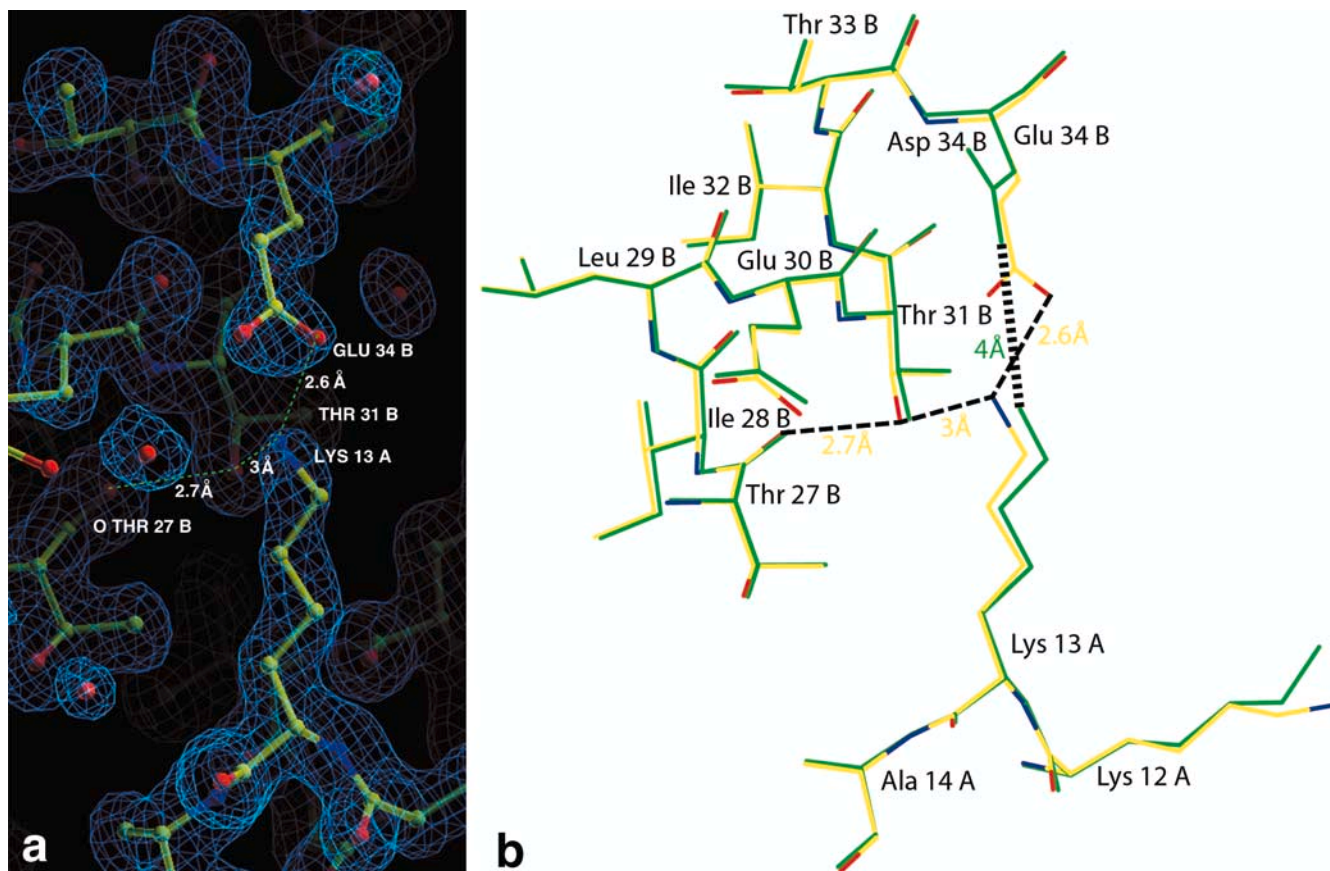


Fig. 4 **a** Electron-density map of HUT mar -E34D mutant. The substitution of the Glu34 with Asp is clearly visible in the electron density. **b** Least-square fit of residues 12–14 of chain A and 27–34 of chain B from the HUT mar -wt structure presented in yellow with residues 12–14 of chain A and 27–34 of chain B from the HUT mar -E34D presented in green

Comparison of the HUT mar and HUB st and IHF structures

In addition to the currently presented crystal structure of HUT mar and its mutant, there are two more solved structures from closely related proteins, i.e., HU protein from *B. stearothermophilus* (HUB st , PDB code 1HUU) and the IHF from *E. coli* (1IHF). At the level of primary structure, the main body of the HUB st proteins can be closely aligned with the HU protein from *T. maritima*, sequence identity 58%, while the sequence identity to IHF is only 36%. The three structures give a reasonable fit despite the moderate sequence identity. Table 7 summarizes the obtained data from the structural comparison among the three proteins.

Discussion

A comprehensive comparison between homologous proteins that display different thermostability is a well-accepted approach to the elucidation of the mechanism of protein thermostability (Kimura et al. 1992; Akasako

et al. 1995; Lehman and Wyss 2001). The structure-mutation approach, despite its limitations, namely, cost and time requirements, remains the predominant method to decipher the mechanism of a protein of interest. As stated in the introduction, our model proteins fulfill the requirements for such an approach. In our previous study, we systematically compared the HU proteins from the thermophilic bacterium *B. stearothermophilus* and the mesophile *B. subtilis*, which differ in 11 out of 90 residues and display a considerable difference in thermal stability. The ΔT_m between the melting temperatures of HUB st and HUB su was determined to be 21.9 °C. A step-by-step, site-directed mutagenesis of all 11 residues in HUB st revealed that the difference in thermostability can be fully accounted for by only three amino acids: Gly15, Glu34, and Val42, which are located in key positions of the molecule (Christodoulou and Vorgias 2002). These three residues are conserved in thermophilic HUs, and their mesophilic counterparts are Glu, Asp, and Ile, respectively. By mutating them to their mesophilic counterparts from *B. subtilis*, we can convert the thermophilic HUB st ($T_m = 61.9$ °C) to its mesophilic homologue HUB su ($T_m = 39.7$ °C). The same amino acid residues in the mesophilic HUB su can be replaced by their thermophilic counterparts, resulting in a thermophilic HUB st -like protein (Christodoulou and Vorgias 2002).

We have extended our studies to the extremophilic HU from *T. maritima*, and in this report we give a

comparison of five HU proteins from microorganisms that optimally grow at temperatures between 30 °C and 80 °C and attempt to decode the structural features involved in their stabilization mechanisms. According to our structural comparisons (Tables 5, 6, 8), the structures of the HU thermophilic *HUBst* and its highly conserved homologue mesophilic *HUBsu* are very similar. The structure of the extremophilic *HUTmar*, described in this report, is very close to *HUBst*, despite only moderate similarity in their primary structures (Esser et al. 1999). No structural data are available for *HUTth* and *HUTvo*. All HU proteins seem to share the same function as DNA-stabilizing proteins, among other auxiliary function(s) described in previous publications referred to in the introduction. The common function and the high structural similarity of the HU proteins make them a very useful model set for detailed structural comparisons, as the observed differences can be expected to be mostly due to thermostability. The ease of comparison is further enhanced by the following features of the HU proteins: HUs contain no Cys residues and no metal(s) or other known cofactors, which can potentially affect the protein thermostability.

In several studies published in the past, it has been shown that higher thermostability is correlated with (1) more Pro, Arg, and Tyr residues (Watanabe et al. 1997; Bogin et al. 1998; Haney et al. 1999; Szilagyi and Zavodsky 2000); (2) fewer Asp, Glu, Cys, and Ser residues (Wright 1991; Cambilliau and Claverie 2000); (3) increased helical content and number of salt bridges, as well as increased polar surface area (Haney et al. 1999; Vogt et al. 1997; Vogt and Argos 1997; Yip et al. 1995; Russell and Taylor 1995; Elcock 1998; Xiao and Honig 1999; Kumar et al. 2000); (4) a larger fraction of residues in α -helices and more Arg and fewer Pro, Cys, and His residues in α -helices (Sternier and Liebl 2001); (5) tighter packing (Eijsink et al. 1992; Jaenicke and Böhm 1998); (6) deletions or shortening of loops (Russell et al. 1997); (7) helical propensities (Querol et al. 1996); and (8) greater hydrophobicity (Haney et al. 1999). From the analysis of the primary structure and the amino acid composition of the five HU molecules shown in Table 1, it is clear that an increase of the charged residues is accompanied by an increase in the T_m of the protein, while the percentage of uncharged residues decreases and the percentage of non-polar residues remains constant. A strong deviation from these correlations can be observed in the case of *HUTvo*. *HUTvo* was previously assigned as a member of the HU family based on its gene sequence as detected in the analysis of the entire genome *T. volcanium*. The genus *Thermoplasma* is unique among archaea, as it is a candidate for the origin of eukaryotic nuclei in the endosymbiosis hypothesis and is adaptable to aerobic and anaerobic environments. This is the only archaeon that grows at temperatures as low as 60 °C whose genome has been sequenced (Kawashima et al. 2000). We are currently working on the elucidation of the structure and function of this HU protein. Among the factors described above, it seems that packing and

salt bridges in HUs are the only structural factors that are significantly related to their thermostability.

The availability of the high-resolution X-ray structures of *HUBst*, *HUTmar*, and *HUTmar*-E45D, as a result of this study, gives us the advantage of mapping the sites of substitutions onto the three-dimensional structure and an opportunity to design mutations that can be examined experimentally. The main body of HU protein, which is responsible for the thermostability of the homodimer, has a high helix content, and it has been shown that most of the differences in amino acid residues are concentrated in the HTH domain, as shown in Table 2, Fig. 1, and Fig. 4. A short turn between the α_2 and α_2 -helix is very important within this domain. Gly15 is situated on the turn between the α_1 - and α_2 -helices. By replacing this residue with its mesophilic counterpart, the geometry of the HTH in *HUTmar* seems to be substantially affected, as the *HUTmar*-G15E mutant has the T_m reduced by -24.7 °C. Furthermore, the replacement of Glu34 with Asp and Val42 with Ile, which are located on the α_2 -helix and β_1 -strand, respectively, also has a moderate destabilizing effect. *HUTmar*-E34D and *HUTmar*-V42I have $\Delta T_m = -7.8$ °C and -9.6 °C, respectively, compared to *HUTmar*-wt ($T_m = 80.5$ °C). By combining these three point mutations, the *HUTmar*-G15E/E34D/V42I has a $T_m = 35.9$ °C, which is very close to its mesophilic homologue. The combined triplet mutation converts the *HUTmar* to its *HUBsu* homologue, which is facilitated by the additive effect of individual mutations.

The structure of the *HUTmar*-E45D mutant clearly demonstrates that a single mutation that abolishes two inter-domain H-bonds can result in a decrease of the thermostability of the wt by nearly 8 °C. According to the X-ray structure of *HUTmar*, a salt bridge is formed between Lys13 of subunit A and Glu34 of subunit B and vice versa (Fig. 4). This interaction cannot take place in *HUBst* and *HUBgl*, since there is a Glu at position 13. Furthermore, Lys13 of the α_1 -helix of one subunit also interacts with Thr27 and Thr31 of the α_2 -helix of the other subunit.

The existence of ion pairs on the surface of the molecule as a factor increasing thermostabilization is in line with the current model of thermostabilization mechanisms, particularly at temperatures close to the boiling point where electrostatic networks are observed to occur in nature on the surface of the molecule (Hensel and Jakob 1994; Karshikoff and Ladenstein 2001).

Although, we have not yet solved the structure of the *HUTmar*-V42I mutant ($\Delta T_m = -9.6$ °C) at high resolution, it is likely that the conservative substitution (Val to Ile) that caused an unexpected destabilization has only a local packing effect. Val-42 in *HUTmar* lies at the beginning of the β_1 -strand in the vicinity of the α_2 -helix. Val-42 is surrounded by the side chains Ala-35, Ile-32, Phe-50, Ile-44, and Met-1, which are highly conserved among HU proteins. All these residues form a very hydrophobic pocket. Val, having a shorter side chain than Ile, provides a more tightly packed core for the

molecule. Introduction of an Ile at this position pushes residue Ile-32, and repulsion between Leu-42 (β_1 -strand) and Ile-32 (α -helix) might occur with a negative effect on the thermostability ($\Delta T_m = -9.6$ °C). This is an interior apolar-to-apolar substitution that alters the packing without an accompanying hydrophobicity change and substantially destabilizes the protein (Sandberg and Terwillinger 1989).

Comparison of the high-resolution three-dimensional structures of HUBst, HUTmar, and HUTmar-E34D shows that the overall differences between the three structures are within the expected coordinate error. Therefore, we looked in detail at the side chain interactions. The differences in the number of salt bridges between the thermophilic and mesophilic homologues appear to correlate with the T_m , while other factors such as compactness and hydrophobicity do not correlate consistently (Karshikoff and Ladenstein 1998).

The information accumulated to date indicates that nature does not rely on a single strategy for thermal stabilization. As a result, many publications in this area arrive at different and sometimes inconsistent conclusions (Wintrode and Arnold 2001). The availability of more complete genome sequences may eventually result in more reliable and accurate estimations of the factors involved, but sequence statistics alone are still unlikely to allow accurate predictions of thermostabilizing mutations (Van den Burg et al. 1998; Haney et al. 1999; Kumar et al. 2000; Lehmann and Wyss 2001).

The somehow puzzling results coming from various analyses lead to the question. Are there general rules to adaptation at high temperature? The answer might be positive, but it is possible that no unambiguous rule can be established and only general principles can be stated. In general, several distinct strategies can be distinguished by which proteins achieve thermostability, but the choice of the strategy employed varies from protein to protein. Our model system concerns small proteins that exhibit high homology and a pronounced difference in thermostability and shows that less than 30% of the amino acid differences in the primary structure are involved in thermostabilization. This is less than 5% of the total residues. This observation highlights the problem of identifying the relevant thermostabilizing mutations, particularly in bigger and more complex proteins.

References

- Akasako A, Haruki M, Oobatake M, Kanaya S (1995) High resistance of *Escherichia coli* ribonuclease HI variant with quintuple thermostabilizing mutations to thermal denaturation, acid denaturation, and proteolytic degradation. *Biochemistry* 34:8115–8122
- Boelens R, Vis H, Vorgias CE, Wilson KS, Kaptein R (1996) Structure and dynamics of the DNA binding protein HU from *Bacillus stearothermophilus* by NMR spectroscopy. *Biopolymers* 40:553–559
- Bogin O, Peretz M, Hacham Y, Korkhin Y, Frolow F, Kalb (Gilboa) AJ, Burstein Y (1998) Enhanced thermal stability of *Clostridium beijerinckii* alcohol dehydrogenase after strategic substitution of amino acid residues with prolines from the homologous thermophilic *Thermoanaerobacter brockii* alcohol dehydrogenase. *Protein Sci* 7:1156–1163
- Broyles SS, Pettijohn DE (1986) Interaction of the *Escherichia coli* HU protein with DNA. Evidence for formation of nucleosome-like structures with altered DNA helical pitch. *J Mol Biol* 187:47–60
- Brünger AT (1992) Free R value: a novel statistical quantity for assessing the accuracy of crystal structures. *Nature* 355:472–475
- Burley SK, Petsko GA (1985) Aromatic-aromatic interaction: a mechanism of protein structure stabilization. *Science* 229:23–28
- Cambilliau C, Claverie JM (2000) Structural and genomic correlates of hyperthermostability. *J Biol Chem* 275:32383–32386
- Castaing BC, Zelwer C, Laval J, Boiteux S (1995) HU protein of *Escherichia coli* binds specifically to DNA that contains single-strand breaks or gaps. *J Biol Chem* 270:10291–10296
- Christodoulou E, Vorgias CE (1998) Cloning, overproduction, purification and crystallization of the DNA binding protein HU from the hyperthermophilic eubacterium *Thermotoga maritima*. *Acta Crystallogr D Biol Crystallogr* 54:1043–1045
- Christodoulou E, Vorgias CE (2002) The thermostability of DNA-binding protein HU from mesophilic, thermophilic, and extreme thermophilic bacteria. *Extremophiles* 6:21–31
- Claret L, Rouvière-Yaniv J (1996) Regulation of HU α and HU β by CRP and FIS in *Escherichia coli*. *J Mol Biol* 263:126–139
- Collaborative Computational Project Number 4 (1994) The CCP4 suite: Programs for protein crystallography. *Acta Crystallogr D Biol Crystallogr* 50:760–763
- Craigie R, Arndt-Jovin, DJ, Mizuuchi D (1985) A defined system for the DNA strand-transfer reaction at the initiation of bacteriophage Mu transposition: protein and DNA substrate requirements. *Proc Natl Acad Sci USA* 82:7570–7574
- Drlica K, Rouvière-Yaniv J (1987) Histone-like proteins of bacteria. *Microbiol Rev* 51:301–319
- Eijsink VG, Dijkstra BW, Vriend G, van der Zee J, Veltman OR, van der Vinne B, van den Burg B, Kempe S, Venema G (1992) The effect of cavity-filling mutations on the thermostability of *Bacillus stearothermophilus* neutral protease. *Protein Eng* 5:421–426
- Elcock AH (1998) The stability of salt bridges at high temperatures: implications for hyperthermophilic proteins. *J Mol Biol* 284:489–502
- Esser D, Rudolph R, Jaeicke R, Böhm G (1999) The HU protein from *Thermotoga maritima*: recombinant expression, purification and physicochemical characterization of an extremely hyperthermophilic DNA-binding protein. *J Mol Biol* 291:1135–1146
- Flashner Y, Gralla JD (1988) DNA dynamic flexibility and protein recognition: differential stimulation by bacterial histone-like protein HU. *Cell* 54:713–721
- French S, Wilson KS (1978) On treatment of negative intensity observations. *Acta Crystallogr A* 34:517–525
- Grove A, Lynette L (2001) High-affinity DNA binding of HU protein from the hyperthermophile *Thermotoga maritima*. *J Mol Biol* 311:491–502
- Haney PJ, Badger JH, Buldak GL, Reich CI, Woese CR, Olsen GJ (1999) Thermal adaptation analyzed by comparison of protein sequences from mesophilic and extremely thermophilic *Methanococcus* species. *Proc Natl Acad Sci USA* 96:3578–3583
- Hensel R, Jakob I (1994) Stability of glycer-aldehyde-3-phosphate dehydrogenase from hyperthermophilic archaea at high temperature. *Syst Appl Microbiol* 16:742–745
- Jaeicke R, Böhm G (1998) The stability of proteins in extreme environments. *Curr Opin Struct Biol* 8:738–748
- Jones TA, Zou JY, Kjeldgaard M (1991) Improved methods for binding protein models in electron density maps and the location of errors in these models. *Acta Crystallogr A* 47:110–119
- Karshikoff A, Ladenstein R (1998) Proteins from thermophilic and mesophilic organisms essentially do not differ in packing. *Protein Eng* 11:867–872
- Karshikoff A, Ladenstein R (2001) Ion pairs and the thermostability of proteins from hyperthermophiles: a “traffic rule” for hot roads. *Trends Biochem Sci* 26:550–556

- Kawamura S, Kakuta Y, Tanaka I, Hikichi K, Kuhara S, Yamasaki N, Kimura M (1996) Glycine-15 in the bend between two α -helices can explain the thermostability of DNA binding protein HU from *Bacillus stearothermophilus*. *Biochemistry* 35:1195–1200
- Kawamura S, Abe Y, Ueda T, Masumoto K, Imoto T, Yamasaki N, Kimura M (1998) Investigation of the Structural Basis for Thermostability of DNA-binding Protein HU from *Bacillus stearothermophilus*. *J Biol Chem* 273:19982–19987
- Kawashima T, Amano N, Koike H, Makino S, Higuchi S, Kawashima-Ohya Y, Watanabe K, Yamazaki M, Kanehori K, Kawamoto T, Nunoshiba T, Yamamoto Y, Aramaki H, Makino K, Suzuki M (2000) Archaeal adaptation to higher temperatures revealed by genomic sequence of *Thermoplasma volcanium*. *Proc Natl Acad Sci USA* 97:14257–14262
- Kimura S, Nakamura H, Hashimoto T, Oobatake M, Kanaya S (1992) Stabilization of *Escherichia coli* ribonuclease hi by strategic replacement of amino acid residues with those from the thermophilic counterpart. *J Biol Chem* 267:21535–21542
- Kraulis PJ (1991) MOLSCRIPT: a program to produce both detailed and schematic plots of protein structures. *J Appl Crystallogr* 24:946–960
- Kumar S, Tsai CJ, Nussinov R (2000) Factors enhancing protein thermostability. *Protein Eng* 13:179–191
- Ladenstein R, Antranikian G (1998) Proteins from hyperthermophiles: stability and enzymatic catalysis close to the boiling point of water. *Adv Biochem Eng Biotechnol* 61:37–85
- Lamzin VS, Wilson KS (1993) Automated refinement of protein models. *Acta Crystallogr D Biol Crystallogr* 49:129–147
- Laskowski RA, MacArthur MW, Moss DS, Thornton JM (1993) PROCHECK: a program to check the stereochemical quality of protein structures. *J Appl Crystallogr* 26:283–291
- Lehmann M, Wyss M (2001) Engineering proteins for thermostability: the use of sequence alignments versus rational design and directed evolution. *Curr Opin Biotech* 12:371–375
- Mensa-Wilmot K, Carroll K, McMacken R (1989) Transcriptional activation of bacteriophage lambda DNA replication *in vitro*: regulatory role of histone-like protein HU of *Escherichia coli*. *EMBO J* 8:2393–2402
- Murshudov GN, Vagin AA, Lebedev A, Wilson KS, Dodson EJ (1999) Efficient anisotropic refinement of macromolecular structures using FFT. *Acta Crystallogr D Biol Crystallogr* 55(1):247–255
- Navaza J (1994) AMoRe: an automated package for molecular replacement. *Acta Crystallogr A* 50:157–163
- Otwinowski Z, Minor W (1997) Processing of X-ray diffraction data collected in oscillation mode. Academic Press, London
- Padas PM, Wilson KS, Vorgias CE (1992) The DNA-binding protein HU from mesophilic and thermophilic bacilli: gene cloning, overproduction and purification. *Gene* 117:39–44
- Perrin S, Gilliland G (1990) Site-specific mutagenesis using asymmetric polymerase chain reaction and a single mutant primer. *Nucleic Acids Res* 18:7433–7438
- Pettijohn DE (1988) Histone-like proteins and bacterial chromosome structure. *J Biol Chem* 263:12793–12796
- Querol E, Perez-Pons JA, Mozo-Villarias A (1996) Analysis of protein conformational characteristics related to thermostability. *Protein Eng* 9:265–271
- Ramachandran GN, Sasisekharan V (1968) Conformation of polypeptides and proteins. *Adv Protein Chem* 23:283–437
- Rice PA, Yang SW, Mizuuchi K, Nash H (1996) Crystal structure of an IHF-DNA complex: a protein-induced DNA U-turn. *Cell* 87:1295–1306
- Rouvière-Yaniv J, Gros F (1975) Characterization of a novel, low-molecular-weight DNA-binding protein from *Escherichia coli*. *Proc Natl Acad Sci USA* 72:3428–3432
- Rouvière-Yaniv J, Yaniv M, Germond J (1979) *E. coli* DNA binding protein HU forms nucleosomal-like structures with double-stranded DNA. *Cell* 17:265–274
- Russell RJ, Taylor GL (1995) Engineering thermostability: lessons from thermophilic proteins. *Curr Opin Biotech* 6:370–374
- Russell RJ, Ferguson JM, Hough DW, Danson MJ, Taylor GL (1997) The crystal structure of citrate synthase from the hyperthermophilic archaeon *Pyrococcus furiosus* at 1.9 Å resolution. *Biochemistry* 36:9983–9994
- Salminen T, Teplyakov A, Kankare J, Cooperman BS, Lahti R, Goldman A (1996) An unusual route to thermostability disclosed by the comparison of *Thermus thermophilus* and *Escherichia coli* inorganic pyrophosphatases. *Protein Sci* 5:1014–1025
- Sandberg WS, Terwilliger TC (1989) Influence of interior packing and hydrophobicity on the stability of a protein. *Science* 245:54–57
- Serrano L, Day AG, Fersht AR (1993) Step-wise mutation of barnase to binase. A procedure for engineering increased stability of proteins and an experimental analysis of the evolution of protein stability. *J Mol Biol* 233:305–312
- Shih P, Kirsch JF (1995) Design and structural analysis of an engineered thermostable chicken lysozyme. *Protein Sci* 4:1063–1072
- Spector S, Wang A, Carp SA, Robblee J, Hendsch ZS, Fairman R, Tidor B, Raleigh DP (2000) Rational modification of protein stability by the mutation of charged surface residues. *Biochemistry* 39:872–879
- Sriprapundh D, Vieille C, Zeikus JG (2000) Molecular determinants of xylose isomerase thermal stability and activity: analysis of thermozymes by site-directed mutagenesis. *Protein Eng* 13:259–265
- Steen IH, Madern D, Karlstrom M, Lien T, Ladenstein R, Birke-land NK (2001) Comparison of isocitrate dehydrogenase from three hyperthermophiles reveals differences in thermostability, cofactor specificity, oligomeric state, and phylogenetic affiliation. *J Biol Chem* 276:43924–43931
- Sterner N, Liebl W (2001) Thermophilic adaptation of proteins. *Crit Rev Biochem Mol Biol* 36:39–106
- Szilagy A, Zavodszky P (2000) Structural differences between mesophilic, moderately thermophilic and extremely thermophilic protein subunits: results of a comprehensive survey. *Struct Fold Des* 8:493–504
- Tanaka I, Appelt K, Dijk J, White SW, Wilson KS (1984) 3-Å resolution structure of a protein with histone-like properties in prokaryotes. *Nature* 310:376–381
- Thompson JD, Gibson TJ, Plewniak F, Jeanmougin F, Higgins DG (1997) The Clustal_X windows interface flexible strategies for multiple sequence alignment aided by quality analysis tools. *Nucleic Acids Res* 25:4876–4882
- Van den Burg B, Vriend G, Veltman OR, Venema G, Eijsink VG (1998) Engineering an enzyme to resist boiling. *Proc Natl Acad Sci USA* 95:2056–2060
- Van Silfhout RG, Hermes C (1995) X-ray instrumentation for a focused wiggler beamline at the EMBL Outstation Hamburg. *Rev Sci Instrum* 66:1818–1820
- Vis H, Mariani M, Vorgias CE, Wilson KS, Kaptein R, Boelens R (1995) Solution structure of the HU Protein from *Bacillus stearothermophilus*. *J Mol Biol* 254:692–703
- Vogt G, Argos P (1997) Protein thermal stability: hydrogen bonds or internal packing? *Fold Des* 2:40–46
- Vogt G, Woell S, Argos P (1997) Protein thermal stability, hydrogen bonds, and ion pairs. *J Mol Biol* 269:631–643
- Watanabe K, Hata Y, Kizaki H, Katsube Y, Suzuki Y (1997) The refined crystal structure of *Bacillus cereus* oligo-1,6-glucosidase at 2.0 Å resolution: structural characterization of proline-substitution sites for protein thermostabilization. *J Mol Biol* 269:142–153
- White SW, Appelt K, Wilson KS, Tanaka I (1989) A protein structural motif that bends DNA. *Proteins* 5:281–288
- White SW, Wilson KS, Appelt K, Tanaka I (1999) The high-resolution structure of DNA-binding protein HU from *Bacillus stearothermophilus*. *Acta Crystallogr D Biol Crystallogr* 55:801–809
- Wilson KS, Vorgias CE, Tanaka I, White SW, Kimura M (1990) The thermostability of DNA-binding protein HU from *Bacillus*. *Protein Eng* 4:11–22

- Wintrode PL, Arnold FH (2001) Temperature adaptation of enzymes: lessons from laboratory evolution. *Adv Protein Chem* 55:161–225
- Wojtuszewski K, Hawkins ME, Cole JL, Mukerji I (2001) HU binding to DNA: evidence for multiple complex formation and DNA bending. *Biochemistry* 27:2588–2598
- Wright HT (1991) Nonenzymatic deamidation of asparaginyl and glutaminyl residues in proteins. *Crit Rev Biochem Mol Biol* 26:4632–4636
- Xiao L, Honig B (1999) Electrostatic contributions to the stability of hyperthermophilic proteins. *J Mol Biol* 289:1435–1444
- Yip KS, Stillman TJ, Britton KL., Artymiuk PJ, Baker PJ, Sedelnikova SE, Engel PC, Pasquo A, Chiaraluce R, Consalvi V (1995) The structure of *Pyrococcus furiosus* glutamate dehydrogenase reveals a key role for ion-pair networks in maintaining enzyme stability at extreme temperatures. *Structure* 3:1147–1158
- Zuber H (1988) Temperature adaptation of lactate dehydrogenase. Structural, functional and genetic aspects. *Biophys Chem* 29:171–179